Original article

Journal of High School Science

Zero-Sum node reconfiguration in a discrete spacetime substrate

Piran S[1], Hisco B[2]

Submitted: April 28, 2026, Revised: version 1, June 15, 2026, version 2, July 14, 2026
Accepted: July 22, 2026

Abstract

The physical origin of late-time cosmic acceleration remains uncertain, motivating investigation of whether a discrete spacetime substrate can reproduce vacuum-like expansion without introducing an explicit cosmological constant. In this work, a phenomenological finite-capacity node model was developed to examine the cosmological consequences of an energy-conserving (zero-sum) discrete substrate and to evaluate its consistency with established cosmological constraints. Alternative dissipative and radiative variants were considered as consistency checks but were found to be incompatible with vacuum-like expansion or existing observational limits. Within the zero-sum framework, local compensation implies a robust k^4-suppressed infrared correction to the primordial spectrum, while the broader blue-scar form was retained as a phenomenological template for small-scale observational testing. Representative realizations of this template were benchmarked against published 21-cm constraints on small-scale primordial power, yielding preliminary bounds on the observationally permissible blue-scar amplitude and turnover scale. Although the framework does not constitute a microscopic derivation of dark energy, the results demonstrate that an energy-conserving discrete-spacetime hypothesis can remain compatible with current cosmological observations while providing a constrained, testable phenomenological signature for future observational studies.

Keywords

Dark energy, Cosmology, Discrete spacetime, Emergent spacetime, Cosmological constant, Primordial power spectrum, Cosmic acceleration, 21-cm cosmology, Gravitational waves, Phenomenological cosmology

---

[1]Corresponding author: Sophia Piran, Emmanuel College, 17 Birmingham Rd, Carrara QLD 4211, Australia. 3030556@students.emmanuel.qld.edu.au
[2]Brayden Hisco, Emmanuel College, 17 Birmingham Rd, Carrara QLD 4211, Australia.bhisco@emmanuel.qld.edu.au

1. Introduction

Late-time cosmic acceleration remains one of the central unresolved problems in cosmology. Observations of Type Ia supernovae established that the expansion of the Universe is accelerating rather than decelerating under the influence of ordinary matter alone (1,2). Subsequent measurements of the cosmic microwave background and large-scale structure supported a concordance cosmology in which the present-day energy budget is dominated by a component with effective equation of state close to $w = -1$ (3-5). At the level of homogeneous expansion, this framework has been observationally successful. Its unresolved difficulty is interpretive: although the standard model reproduces the observed background behavior, it does not uniquely identify the physical origin of the vacuum-like sector responsible for the acceleration (3-5).

The simplest description is a cosmological constant, introduced as a uniform energy density that does not dilute as the Universe expands (6). Although this reproduces the observed background history, it also raises longstanding theoretical questions concerning fine-tuning and the physical interpretation of vacuum energy (3,5,6). These tensions have motivated a broad range of alternatives, including dynamical dark-energy models, modified-gravity frameworks, and approaches in which large-scale spacetime geometry may emerge from more microscopic structure rather than being fundamental in the continuum sense (3,4,7). Within that broader context, it becomes natural to ask whether a vacuum-like cosmological sector could arise not from an explicit cosmological constant, but from a constrained reconfiguration process operating within an effective discrete substrate.

Several developments in theoretical physics support the possibility that spacetime may admit a deeper microscopic description. Black-hole thermodynamics established a close connection between geometry, entropy, and information at fundamental scales (8,9). Holographic arguments further suggested that spacetime may possess a finite underlying capacity rather than behaving as an unconstrained continuum at arbitrarily small distances (10,11). Related approaches, including causal-set and emergent-spacetime frameworks, have explored how effective geometric behavior may arise only after coarse-graining over microscopic degrees of freedom (10–12). These lines of work do not determine a model of cosmic acceleration by themselves, but they motivate the present question: whether a discrete substrate with finite local capacity can remain compatible with the observed vacuum-like background while satisfying existing cosmological consistency conditions.

The framework examined in the present study was explicitly phenomenological. Spacetime was represented as a finite-capacity node ensemble in which cosmological expansion corresponded to an increase in geometric capacity through node reconfiguration. Within such a framework, the large-scale behavior depended on how local stress was converted into new structure, and this immediately imposed a stringent bookkeeping problem. Dissipative node creation drove the effective dark-energy sector away from vacuum-like behavior. Strong coupling to photons generated spectral distortions of the cosmic microwave background. Strong coupling to the gravitational sector generated an excessive stochastic gravitational-wave background. The scientific content of the framework therefore lay not in the freedom to posit many branches, but in the fact that most simple branches were excluded once background, thermal, and radiative consistency conditions had been imposed.

A background match alone, however, would not have made such a framework scientifically useful. If the surviving branch merely reproduced the standard ΛCDM expansion history with no residual consequence, it would have amounted only to a reformulation of an already successful background law. For that reason, the present study also examined whether a discrete substrate could leave a distinct primordial imprint. Because a compensated node-reconfiguration event was treated as local, it could not inject unsuppressed long-wavelength power into the metric. This locality requirement forced the leading correction to the primordial spectrum to be infrared-suppressed, with the most robust contribution scaling as k^4 at small wavenumber. Beyond that infrared limit, the broader blue-scar structure was treated not as a first-principles microscopic prediction, but as a phenomenological template whose detailed turnover and modulation would require a more complete substrate theory.

Because such a template modifies the primordial spectrum on small scales, theoretical consistency alone would not have been sufficient. A viable phenomenological signature must also remain compatible with existing observational limits on excess small-scale primordial power. The present study therefore supplemented the consistency analysis with a limited comparison against published 21-cm constraints on small-scale primordial power (13). The purpose of that comparison was not to construct a full cosmological likelihood analysis, but to determine whether representative blue-scar realizations admitted an observationally permissible parameter space within the phenomenological framework considered here.

The conceptual interpretation adopted throughout was correspondingly restrained. The zero-sum branch was not treated as a microscopic event-by-event conservation law, but as an effective coarse-grained closure selected by consistency. In that respect, the framework may be viewed as structurally analogous to a constrained thermodynamic system, in which macroscopic viability emerges only within restricted regimes defined by competing microscopic tendencies (14,15). Dissipative node creation, thermal coupling, and gravitationally radiative leakage acted as channels that displaced the system from observational admissibility, whereas the zero-sum limit represented the only branch that remained compatible with a vacuum-like background once those competing constraints had been imposed. This interpretation did not constitute a thermodynamic derivation of cosmology; rather, it provided a statistical and phenomenological way to understand why a macroscopically compensated regime could emerge even if the underlying microscopic realizations were locally heterogeneous.

The analysis therefore addressed three linked questions: whether any effective branch of the discrete-substrate framework remained compatible with a vacuum-like background, whether the surviving branch avoided thermal and radiative inconsistency, and whether its residual blue-scar signature was both observationally permissible and observationally testable. Within the class of models examined, the significance of the framework did not lie in replacing standard cosmology at the homogeneous level, but in isolating a narrowly constrained discrete-substrate regime whose small-scale signature could be confronted with existing bounds and future high-k observations.

2. Materials and Methods

2.1 Model framework

A phenomenological discrete-substrate framework was constructed in which the effective dark-energy sector was represented by a node population embedded in an expanding Friedmann-Robertson-Walker background. The node-sector density was written as, $\rho_N(a)=\frac{u_* N(a)}{V(a)}$, where u_* denoted the structural energy per node, $N(a)$ denoted the node count in a physical region, and $V(a) \propto a^3$ denoted the physical volume. The effective fluid was required to satisfy the continuity equation, $\dot{\rho}_N+3H(\rho_N+P_N)=0, H\equiv\frac{\dot{a}}{a}$. In the zero-sum closure, the physical node density was assumed to remain constant under expansion, $\frac{N(a)}{V(a)}=const$, so that $\rho_N(a) \propto a^0$. Within the effective description adopted here, this condition implied, $P_N=-\rho_N, w_N\equiv\frac{P_N}{\rho_N}=-1$. This assumption defined the coarse-grained closure tested in the present study and was not interpreted as a microscopic event-by-event conservation law. Rather, it was adopted to test phenomenological admissibility under benchmark cosmological constraints. A broader parameterized branch was also examined using $w=-1+2p(1-r)$, where p represented the sensitivity of reconfiguration to local saturation and r represented the fraction of local stress converted directly into structural node formation.

2.2 Core model assumptions and scope

The analytical framework rested on four explicit phenomenological assumptions. First, individual nodes were treated as effective coarse-grained degrees of freedom rather than as fundamental quantum-gravitational entities. Second, the zero-sum closure was evaluated as a macroscopic consistency condition selected to maintain compatibility with benchmark background constraints, rather than as a derivation from a microscopic action. Third, the functional form of the primordial blue-scar correction beyond the robust k^4 infrared scaling was treated as a phenomenological template for falsification rather than as an exact microscopic prediction. Fourth, the observational metrics used throughout the analysis were treated as benchmark consistency tests against existing cosmological limits rather than as a full multi-parameter likelihood exploration of cosmological parameter space.

These assumptions were adopted to test phenomenological admissibility within an effective framework rather than to claim a completed microscopic theory of spacetime. The resulting conclusions should therefore be interpreted as consistency-selection statements, not as first-principles derivations. The branch comparison was not exhaustive over all conceivable discrete-substrate constructions, and all exclusion statements in this study apply only to the explicitly parameterised closures and coupling channels examined here.

2.3 Background evolution calculations

Background evolution was evaluated for three branches of the model: a dissipative branch, a partially compensated branch, and the zero-sum branch. For the dissipative model, the node-creation law was written as, $\frac{dN}{dt}=\alpha N\eta^{p}$, with $\eta=\frac{E}{CN},\dot{E}=-\epsilon\dot{N}$, where η denoted the saturation ratio, E denoted the orbital-energy reservoir, C denoted node capacity, and ϵ denoted the positive creation cost. The representative dissipative run used $p=0.14$, $\eta_0=0.85$, and $\frac{\epsilon}{C}=0.085$.

For the partially compensated branch, the effective node-sector equation of state was evaluated using $p=0.14$, $r=0.93$, $\Omega_{m0}=0.315$, and $\Omega_{N0}=0.685$. The zero-sum branch was obtained by setting $r=1$, which yielded the effective closure $w_N=-1$ within the adopted coarse-grained description. For comparison with the standard background, the dimensionless expansion history was computed as,

$$E(z)\equiv\frac{H(z)}{H_0}=\left[\Omega_{m0}(1+z)^3+\Omega_{N0}(1+z)^{3(1+w_N)}\right]^{\frac{1}{2}},$$

with $w_N=-1$ for the zero-sum branch and $w_N=-0.9804$ for the representative partially compensated branch. The luminosity distance was written as, $D_L(z)=\frac{(1+z)c}{H_0}\int_0^z\frac{dz'}{E(z')}$, and the corresponding distance modulus was, $\mu(z)=5\log_{10}\left(\frac{D_L(z)}{Mpc}\right)+25$. This quantity was used to quantify background residuals relative to the ΛCDM baseline.

2.4 Spectral-distortion bookkeeping

Thermal quietness was assessed by introducing a photon branching fraction f_γ, defined as the fraction of reconfiguration energy transferred to the photon bath. The effective photon-coupled power was modeled as, $Q_\gamma=f_\gamma\,3H(1+w_N)\rho_N$. The fractional energy injection into the microwave background was then integrated over the standard distortion eras. For the μ-era and y-era, small-distortion estimates were used, $\mu\approx1.4\frac{\Delta\rho_\gamma}{\rho_\gamma},y\approx\frac{1}{4}\frac{\Delta\rho_\gamma}{\rho_\gamma}$.

The resulting amplitudes were compared against the adopted COBE/FIRAS limits, $|\mu|<9\times10^{-5}$ and $|y|<1.5\times10^{-5}$. The maximum allowed f_γ was determined by requiring the predicted distortion to remain below these bounds. Under this construction, the spectral-distortion analysis functioned as a consistency filter on thermally coupled branches rather than as a complete thermal history model.

2.5 Gravitational-wave bookkeeping

The effective gravitational-wave source term was evaluated exclusively for parameterized branches deviating from the exact zero-sum limit, $w_N\neq-1$. In the exact zero-sum closure, the source term vanished identically, so the ideal branch itself was radiation-silent. The gravitational-wave calculation therefore served as an exclusion test for non-ideal radiative leakage rather than as a source model for the exact zero-sum branch.

The effective gravitational-wave density obeyed $\frac{d\rho_{gw}}{d\ln a}+4\rho_{gw}=3f_{gw}(1+w_N)\rho_N$. This equation was integrated numerically to obtain the present-day background density $\Omega_{gw,0}$ and the scaled quantity $\Omega_{gw,0}\ h^2$. The early-universe impact was estimated through the radiation-equivalent proxy $\Delta N_{eff}\propto\frac{\rho_{gw}}{\rho_{rad}}$, evaluated at recombination and at a representative Big Bang nucleosynthesis epoch. The resulting background was compared with the adopted integrated energy-density bound reported in the cited gravitational-wave constraints, and the largest allowed f_{gw} was obtained by requiring the model output to remain below that threshold.

2.6 Primordial source model

The primordial correction was modeled by treating each node-reconfiguration event as a localised stochastic source $s(x,\tau)$ with support on a finite correlation domain of characteristic size L_*. Local compensation was imposed by requiring the monopole and dipole moments to vanish, $\int d^3x\ s(x,\tau)=0, \int d^3x\ x_i\ s(x,\tau)=0$. The Fourier transform of the source was expanded for $kL_*\ll 1$, yielding $s(k,\tau)=-\frac{1}{2}k_ik_jQ^{ij}(\tau)+O(k^3)$, where Q^{ij} was the second moment of the source. This expansion established the infrared scaling $s(k)=O(k^2)$, and therefore $P_{node}(k)\propto k^4$ for the corresponding node-sector power. The total primordial spectrum was parameterized as $P_\zeta(k)=P_{infl}(k)\left[1+\Delta_{node}(k)\right]$, with the node correction written as,

$$\Delta_{node}(k)=A_n\left(\frac{k}{k_s}\right)^4W^2\left(\frac{k}{k_d}\right)\left[1+\beta\cos\left(\omega\ln\frac{k}{k_s}+\phi\right)\right].$$

A Gaussian ultraviolet regulator, $W(x)=e^{-x^2}$, was used in the representative plots. Here A_n denoted the correction amplitude, k_s the reference scale, k_d the turnover scale, β the modulation amplitude, ω the logarithmic frequency, and ϕ the phase. Within the present study, the robust prediction was the infrared k^4 behavior implied by locality and compensation, whereas the detailed turnover and modulation structure remained phenomenological.

2.7 Preliminary observational comparison with 21-cm small-scale constraints

To place the blue-scar template against an existing observational benchmark, a limited comparison was performed with the 21-cm global-signal constraints derived by Yoshiura et al. (13). That analysis reported strong sensitivity to excess primordial power over the band $10<k<10^2\,Mpc^{-1}$, with substantially weaker sensitivity over $10^2<k<10^3\,Mpc^{-1}$, and emphasized that the resulting bounds depend on fiducial astrophysical assumptions such as M_{turn}, L_X, and the adopted filtering prescription. The present comparison was therefore interpreted as a preliminary consistency benchmark rather than a full likelihood constraint.

For this purpose, the oscillatory modulation was switched off by setting $\beta=0$, so that the comparison was made against the smooth envelope of the template rather than against phase-dependent local oscillations. The reference scale was fixed at $k_s=10\,Mpc^{-1}$, aligning the onset of the phenomenological correction with the lower edge of the directly constrained small-scale interval. Under these representative choices, the correction reduced to, $\Delta_{node}(k)=A_n\left(\frac{k}{10\,Mpc^{-1}}\right)^4 \exp\,[-2\left(\frac{k}{k_d}\right)^2]$.

A conservative admissibility criterion was then imposed by requiring $1+\Delta_{node}(k)\leq 10$ for $10<k<10^2\,Mpc^{-1}$, so that representative realizations remained below the published upper envelope associated with the benchmark $p_1 \lesssim 10$ limit. This criterion defined the allowed region in the (A_n, k_d) plane reported in the Results section.

2.8 Numerical implementation and figure generation

All numerical integrations, parameter sweeps, and visualisation routines were performed using custom-written MATLAB scripts developed specifically for this study. Background differential equations were integrated numerically on uniform or logarithmic redshift grids depending on the convergence requirements of the quantity under evaluation. The representative distributions for the equation-of-state evolution, the compensated blue-scar spectrum, the residual logarithmic modulation, and the observational admissibility region in (A_n, k_d) space were generated directly from the model equations stated above. The scripts used to produce the manuscript outputs were archived and can be accessed in an external repository (see Code availability) to ensure reproducibility.

2.9 Model outputs and reporting

Because the study consisted of deterministic analytical and numerical evaluations of a defined model rather than repeated experimental measurements, exact model outputs, residuals, and threshold values were reported instead of p-values for most calculations. Quantities such as $w(z)$, $\Delta\mu(z)$, $\Omega_{gw,0}h^2$, and the coupling bounds on f_γ and f_{gw} were obtained directly from the model integrations and reported numerically in the Results section. The observational benchmark comparison likewise yielded explicit amplitude-turnover admissibility conditions rather than statistical confidence contours from a full survey likelihood. Figure and table references were used to connect each reported quantity to the corresponding visualisation or summary output.

3. Results and Discussion

3.1 Dissipative node creation was incompatible with a vacuum-like background

The dissipative branch was first evaluated to determine whether a substrate with a positive net creation cost could remain compatible with vacuum-like expansion. Any viable node-reconfiguration framework had to keep the effective equation of state close to the observed vacuum-like regime over the late-time cosmological interval. The dissipative branch failed this requirement. For the representative case with sensitivity exponent $p=0.14$, initial saturation $\eta_0=0.85$, and normalized creation cost $\frac{\epsilon}{C}=0.085$, the effective equation of state was $w(0)=-0.692$, $w(1)=-0.717$, and $w(2)=-0.719$. Under the same assumptions, the inferred dark-energy proxy changed sign at $z\approx 0.724$, indicating that this branch did not maintain a physically acceptable late-time vacuum sector. Within the class of models examined, dissipative node creation therefore displaced the substrate too far from the vacuum-like regime to remain background-viable (Table 1).

Table 1. Selection criteria for discrete-substrate variants. Dissipative, thermal, and radiative branches were excluded by background, spectral-distortion, and stochastic-background constraints, respectively. Among the variants examined, the zero-sum limit was the only branch retained.

Variant	Mechanism	Conflict	Status
Dissipative substrate ($r<1$)	Internal energy loss during node formation	$w>-1$; background departs from vacuum-like behavior	Excluded
Thermal substrate ($f_\gamma>0$)	Latent energy dumped into photons	Excess spectral distortion	Excluded as a generic branch
GW-radiative substrate ($f_{gw}>0$)	Latent energy emitted as stochastic GWs	Excess late-time stochastic background	Excluded as a generic branch
Zero-sum substrate ($r=1$, $f_\gamma\approx 0, f_{gw}\approx 0$)	No large dissipative exhaust	$w=-1$ at background level	Survives preliminary consistency checks

3.2 Partial compensation improved the background fit but did not remove the bookkeeping problem

A partially compensated branch was then evaluated to determine whether the benchmark background could be reproduced more closely than in the dissipative case. A two-fluid background containing matter and a node sector was evolved using $\Omega_{m0}=0.315$, $\Omega_{N0}=0.685$, $p=0.14$, and $r=0.93$, and the result was compared with the corresponding ΛCDM baseline. This branch tracked the benchmark background substantially better than the dissipative branch. The node sector reached $w_N=-0.9804$, and the present-day deceleration parameter was $q_0=-0.507$. Over the interval $0\le z\le 2$, the maximum fractional deviation in $H(z)/H_0$ relative to the baseline was $0.486\,\%$, while the maximum distance-modulus residual was $8.25\times 10^{-3}\ mag$. At $z=1$, the distance-modulus residual was $-8.11\times 10^{-3}\ mag$, and matter-node equality occurred at $z\approx 0.303$. These results showed that partial compensation could mimic the homogeneous background well, but not exactly, and still required a nontrivial energy-release channel.

3.3 The zero-sum closure was the only effective branch consistent with a vacuum-like homogeneous sector

The zero-sum closure was then imposed to determine whether any coarse-grained branch could remain degenerate with a vacuum-like background while satisfying the preceding consistency filters. In this closure, the physical node density was held constant under expansion, so that the node-sector density remained independent of the scale factor.

Substitution into the continuity equation then yielded the effective relation $P_N = -\rho_N$, corresponding to $w_N = -1$. Across the sampled redshift range, the zero-sum branch remained degenerate with the homogeneous ΛCDM vacuum sector, and the effective equation of state remained flat at $w = -1$ (Figure 1). Within the class of closures examined, these results identified the zero-sum limit as the only effective branch that remained compatible with a vacuum-like homogeneous background while satisfying the imposed consistency conditions. This conclusion was interpreted at the coarse-grained level of the phenomenological framework rather than as a microscopic event-by-event law.

3.4 Photon-coupled reconfiguration was tightly constrained by spectral-distortion bookkeeping

The thermal quietness of the surviving branch was then tested by introducing a photon branching fraction f_γ and estimating the resulting μ-type and y-type spectral distortions. Any viable substrate had to avoid depositing detectable heat into the cosmic microwave background. The early-universe distortions were negligible: the μ-era contribution scaled as $7.92 \times 10^{-17} f_\gamma$, and the pre-recombination y-era contribution scaled as $4.78 \times 10^{-11} f_\gamma$. The dominant constraint arose after recombination, where the effective y-distortion scaled as $46.93 f_\gamma$. Requiring the predicted distortion to remain below the adopted observational limit imposed $|f_\gamma| \lesssim 3.2 \times 10^{-7}$. Generic thermally coupled branches were therefore excluded, and any surviving node-reconfiguration channel had to remain effectively adiabatic with respect to the photon sector (Table 1).

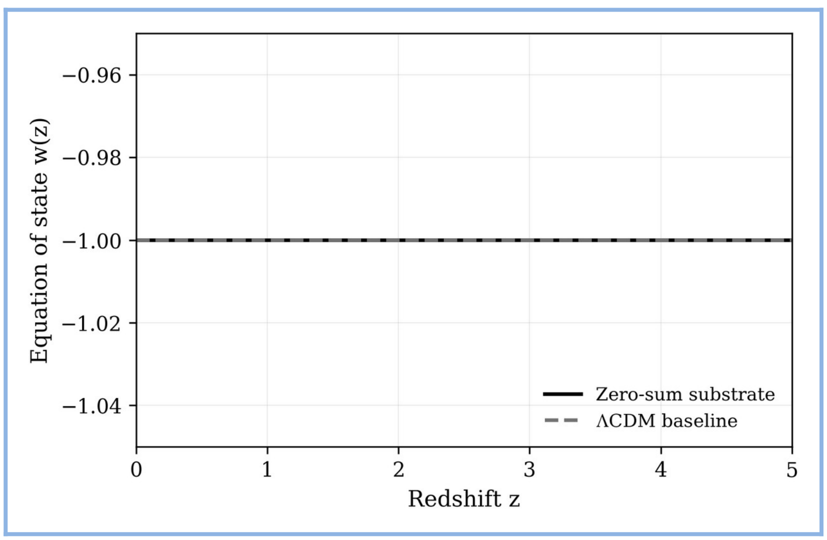

Figure 1. Effective equation of state of the zero-sum substrate. The zero-sum branch remained degenerate with the ΛCDM background, yielding w = -1 at the homogeneous level.

3.5 Radiative leakage into gravitational waves excluded nearby non-ideal branches

The gravitational-wave bookkeeping calculation was evaluated only for parameterized branches deviating from the exact zero-sum closure. In the exact $w_N = -1$ limit, the source term vanished identically, so the ideal branch itself remained radiation-silent.

The purpose of the calculation was therefore not to predict gravitational radiation from the exact zero-sum branch, but to determine how strongly nearby non-ideal branches were constrained by radiative leakage. For unit coupling in the non-ideal parameterized branch, the present-day stochastic background reached $\Omega_{gw,0} = 1.02 \times 10^{-2}$ and $\Omega_{gw,0} h^2 = 4.64 \times 10^{-3}$, far above the adopted integrated bound. By contrast, the early-universe contribution remained negligible, with $\Delta N_{eff}(z \approx 1100) = 8.49 \times 10^{-10} f_{gw}$ and $\Delta N_{eff}(z \approx 10^9) = 2.80 \times 10^{-33} f_{gw}$. The dominant limit therefore arose from late-time accumulation rather than from the radiation era. Requiring the present-day background to remain below the adopted threshold imposed $|f_{gw}| \lesssim 1.2 \times 10^{-3}$. Generic gravitationally radiative branches were therefore excluded, and the surviving substrate had to remain both thermally quiet and gravitationally quiet (Table 1).

3.6 Local compensation determines the infrared structure of the primordial correction

The primordial signature of a local, compensated node-reconfiguration event was then evaluated. The source was modelled as a stochastic perturbation with vanishing monopole and dipole moments, and its Fourier transform was expanded in the infrared limit. Because the monopole and dipole terms cancelled, the leading nonzero contribution scaled as k^2 as $k \to 0$. The corresponding node-sector contribution to the power spectrum therefore scaled as k^4 in the infrared. The total curvature spectrum was then parameterized as a baseline inflationary spectrum multiplied by a node-induced correction with a smooth ultraviolet regulator and optional logarithmic modulation. Under this construction, the correction remained negligible at low k, rose as k^4 at intermediate wavenumber, and turned over at the regulator scale (Figure 2).

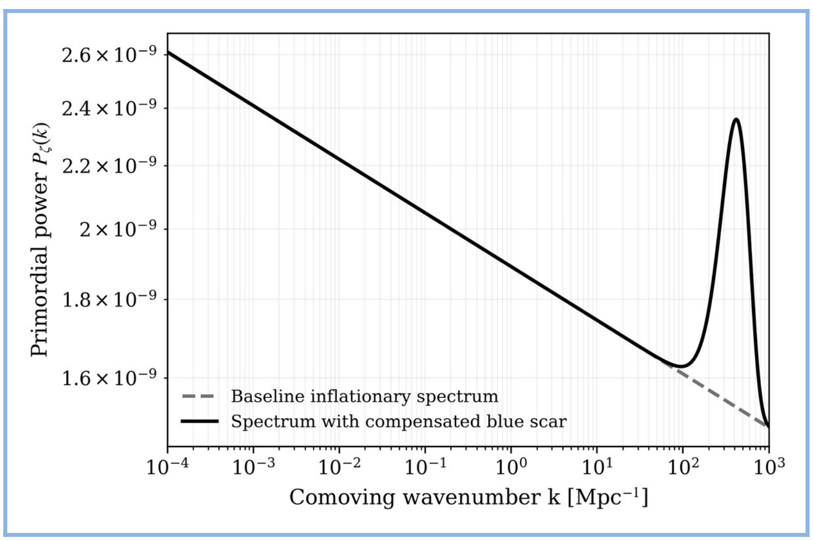

Figure 2. Compensated blue correction to the primordial spectrum. The node-sector contribution was infrared-suppressed by local compensation, rose as k^4, and was regulated by a smooth ultraviolet cutoff at kd.

The residual modulation relative to the baseline spectrum remained small on large scales and became structured only in the high-k regime, where future high-resolution surveys would be most sensitive (Figure 3). Within the framework examined here, the robust result was therefore the infrared k^4 suppression implied by locality and compensation, whereas the broader blue-scar form beyond that limit was retained only as a phenomenological template.

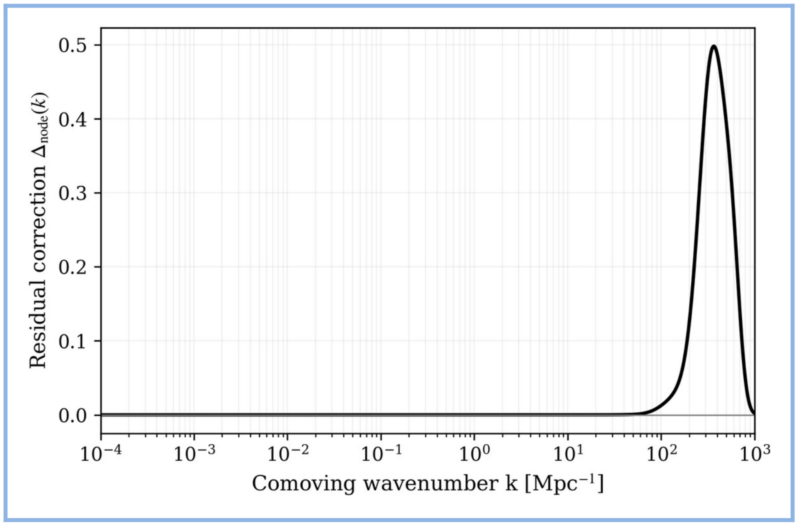

Figure 3. Residual spectrum relative to the baseline ΛCDM prediction. The optional logarithmic modulation parameterized a possible microscopic cadence in node reconfiguration during horizon exit.

3.7 Preliminary observational bounds on the blue-scar template

To move beyond a purely qualitative prediction, representative blue-scar realizations were benchmarked against the 21-cm global-signal constraints of Yoshiura et al., who showed under fiducial astrophysical assumptions that the small-scale primordial enhancement factor is bounded approximately by $p_1 \lesssim 10$ over $10 < k < 10^2\, Mpc^{-1}$, while the sensitivity is substantially weaker over $10^2 < k < 10^3\, Mpc^{-1}$; in a single broad-bin parametrisation over $10 < k < 10^3\, Mpc^{-1}$, they reported the preliminary range $2 \lesssim p_3 \lesssim 8$. The same study emphasized that these limits depend on astrophysical assumptions such as M_{turn}, L_X, and the adopted filtering procedure, and should therefore be interpreted as preliminary consistency benchmarks rather than definitive exclusions.

For the present benchmark comparison, the oscillatory modulation was set to zero, $\beta = 0$, so that the observational test was performed against the smooth blue-scar envelope rather than against phase-dependent local oscillations. The reference scale was fixed at $k_s = 10\, Mpc^{-1}$, aligning the onset of the phenomenological correction with the lower edge of the directly constrained small-scale band. Under these representative choices, the node-induced correction reduced to, $\Delta_{node}(k) = A_n \left(\frac{k}{10\, Mpc^{-1}}\right)^4 \exp\left[-2\left(\frac{k}{k_d}\right)^2\right]$. A conservative observational admissibility criterion was then imposed by requiring $1 + \Delta_{node}(k) \leq 10$ for $10 < k < 10^2\, Mpc^{-1}$, so that the template remained below the published upper envelope associated with the $p_1 \lesssim 10$ constraint. This yielded the preliminary bound,

$$A_n \le \begin{cases} 9\,\exp\left[2\left(\frac{10}{k_d}\right)^2\right], & k_d < 10\,Mpc^{-1}, \\ 66.5\left(\frac{10}{k_d}\right)^4, & 10 \le k_d \le 100\,Mpc^{-1}, \\ 9\times10^{-4}\,\exp\left[2\left(\frac{100}{k_d}\right)^2\right], & k_d > 100\,Mpc^{-1}. \end{cases}$$

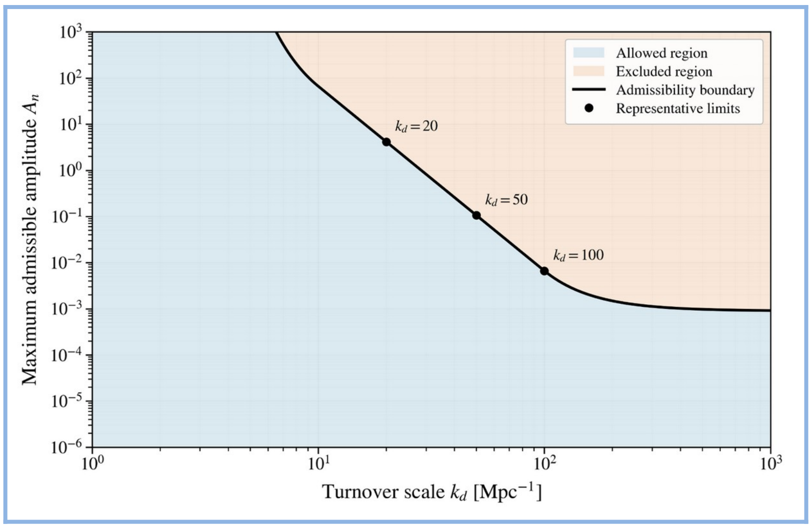

Figure 4. Preliminary observational admissibility region for the blue-scar template in the (A_n, k_d) plane. The allowed region was defined by requiring the smooth node-induced correction to remain below the adopted 21-cm benchmark over $10 < k < 10^2\ Mpc^{-1}$.

The admissible region was therefore strongly correlated rather than rectangular (Figure 4). Large amplitudes remained allowed only when the turnover occurred sufficiently early, so that the enhancement was already exponentially regulated within the observationally constrained band. By contrast, later turnover forced the blue-scar amplitude to become rapidly small. Representative limits were,

$$A_n \lesssim 4.16\left(k_d = 20\,Mpc^{-1}\right), A_n \lesssim 1.06\times10^{-1}\left(k_d = 50\,Mpc^{-1}\right), A_n \lesssim 6.65\times10^{-3}\left(k_d = 100\,Mpc^{-1}\right).$$

Within this benchmarked envelope analysis, the blue-scar template therefore remained observationally permissible, but only within a restricted amplitude-turnover corridor. In this limited but nontrivial sense, the phenomenological signature ceased to be merely qualitative and acquired a first preliminary observationally constrained parameter regime.

3.8 Statistical locality as the motivation for Zero-Sum redistribution

A further motivation for the zero-sum formulation arises from the statistical interpretation of the discrete substrate. The present framework is not intended to imply that every microscopic node undergoes identical evolution or that energy redistribution is coordinated globally in a deterministic manner. Rather, it is conceptually analogous to statistical thermodynamics, in which macroscopic equilibrium emerges from many local interactions while individual microscopic states remain heterogeneous, stochastic, and potentially metastable.

Under this interpretation, newly created spacetime nodes need not be assigned a universally fixed vacuum-like energy density at the moment of formation. Instead, node creation may be understood as being accompanied by local redistribution among neighbouring substrate elements. Individual exchange events may vary substantially in magnitude and configuration, yet the collective behavior of many such interactions can still yield an effectively compensated macroscopic sector. The zero-sum condition is therefore interpreted not as an exact microscopic update rule imposed on every node, but as an emergent coarse-grained constraint.

This interpretation contrasts with an alternative discrete prescription in which each newly created node is assumed to carry precisely the vacuum-like energy density required to reproduce the ΛCDM background. Such a construction is not mathematically excluded, but it amounts to positing a uniform microscopic assignment rule whose physical origin lies outside the local substrate dynamics. By contrast, the zero-sum formulation may be understood in terms of local exchange and statistical emergence, so that the compensated macroscopic sector arises from many locally varying microscopic interactions rather than from an externally imposed uniform creation rule.

Within the phenomenological framework examined here, this does not establish zero-sum redistribution as a unique microscopic truth. Rather, it clarifies why the surviving branch may be regarded as the most economical effective closure among the cases considered: it requires only local interactions, admits heterogeneous microscopic realizations, and reproduces the compensated vacuum-like behavior selected by the imposed consistency conditions.

3.9 The surviving branch was best interpreted as a constrained coarse-grained admissibility condition

Taken together, these results showed that the discrete-substrate framework did not remain viable in its most general form. Dissipative, thermally coupled, and gravitationally radiative branches were systematically excluded once background, spectral-distortion, and stochastic-background constraints had been imposed. The value of the surviving branch therefore arose from restriction rather than freedom. The zero-sum closure was not retained as an arbitrary tuning, but as the only phenomenologically admissible coarse-grained regime remaining after nonviable branches had been removed.

This interpretation was strengthened by the thermodynamic and statistical framing introduced in response to review. In constrained thermodynamic systems, macroscopic viability emerges only within restricted parameter regimes defined by competing tendencies rather than from any single contribution in isolation. The present framework could be construed to exhibit a conceptually similar structure. Dissipative node creation, thermal coupling, and gravitationally radiative leakage acted as competing channels that displaced the cosmological sector from observational admissibility, whereas the zero-sum limit represented the only coarse-grained regime in which those competing contributions remained globally balanced. In this interpretation, the surviving branch was not selected because it was aesthetically simple, but because it alone remained phenomenologically admissible once the imposed consistency conditions had been enforced (section 3.8). The compensated high-k blue-scar correction was therefore naturally interpreted as a residual ultraviolet signature of the underlying microscopic substrate, analogous to the way macroscopic thermodynamic behavior can retain indirect traces of microscopic statistical structure.

The statistical interpretation also removed the appearance of artificial exactness. In statistical thermodynamics, a system may satisfy a globally favourable free-energy condition while still permitting heterogeneous local kinetics, metastable configurations, and microscopic fluctuations. The present framework admitted a conceptually similar reading. The zero-sum condition did not require every microscopic node-reconfiguration event to be individually identical or perfectly balanced in isolation; rather, it functioned as an effective coarse-grained constraint across an ensemble of local substrate realizations. Different microscopic regions could therefore support differing local reconfiguration dynamics while still collectively preserving the globally compensated, vacuum-like expansion required by cosmological observations. Under this framing, the observed background corresponded not to rigid microscopic uniformity, but to an emergent macroscopic admissibility condition arising from heterogeneous underlying dynamics.

A model that matched the homogeneous background alone would nevertheless have had limited scientific value. If the zero-sum branch had been exactly degenerate with ΛCDM in all observables, it would have amounted only to a reinterpretation of a known background law. The scientific value of the framework therefore lay not in reproducing $w = -1$ by itself, but in identifying a residual signature that survived the imposed consistency filters. Once node reconfiguration was required to be local and compensated, the leading infrared contribution became k^4, ensuring that the substrate remained silent on large scales while still permitting structured small-scale deviations. The compensated blue scar was therefore the main falsifiable consequence of the framework, and the preliminary 21-cm comparison showed that this consequence remained observationally viable only within a restricted amplitude-turnover corridor.

Several limitations remained. First, the model was phenomenological rather than microscopic: no underlying Hamiltonian, path integral, or quantum-gravitational action had been derived for the node-cleave process. Second, the observational tests were benchmark consistency checks rather than full likelihood analyses against modern survey data. Third, the detailed turnover scale, amplitude, and modulation structure of the blue scar remained phenomenological beyond the robust infrared limit and would require a more complete microscopic theory before the model could be treated as predictive in a stronger sense. Additional work would therefore be required to embed the template into full cosmological inference pipelines, including high-multipole cosmic microwave background analyses, weak-lensing measurements, galaxy clustering, and 21-cm probes of small-scale primordial structure.

Within those limitations, however, the framework still accomplished something nontrivial. It converted a discrete-substrate approach to cosmic acceleration from unconstrained speculation into a consistency-selection problem with an explicit surviving branch and a falsifiable residual signal. The principal contribution was not a proof that spacetime is discrete, nor a derivation of dark energy from first principles, but the identification of a narrowly constrained phenomenological regime that remained macroscopically viable while leaving a structured small-scale signature that is both observationally falsifiable and already preliminarily benchmarked against existing 21-cm constraints.

4. Conclusion

This study investigated the cosmological implications of a phenomenological zero-sum discrete-spacetime framework as a possible description of vacuum-like cosmic acceleration. Rather than deriving the microscopic origin of dark energy, the analysis examined whether an energy-conserving discrete substrate could remain compatible with existing cosmological observations while producing distinctive observational consequences. Consistency checks confirmed that dissipative or radiative variants do not reproduce the required vacuum-like behavior, reinforcing the adoption of the zero-sum formulation as the phenomenological framework considered throughout this work.

Within this framework, locality and compensation imply a robust infrared k^4 suppression together with a phenomenological blue-scar modification of the primordial power spectrum. Comparison with published 21-cm constraints demonstrates that these signatures remain observationally viable only within a restricted region of parameter space, providing an initial benchmark for future observational tests.

The principal contribution of this work is therefore not the derivation of a fundamental theory of dark energy, but the formulation and preliminary observational assessment of a discrete-spacetime phenomenology whose predictions can be quantitatively tested as increasingly sensitive measurements of small-scale cosmological structure become available. Future work should derive the zero-sum dynamics from a microscopic theory, establish whether the predicted spectral modifications arise uniquely from the underlying physics, and perform comprehensive Bayesian inference using multiple cosmological probes to determine whether this phenomenological framework offers measurable advantages over the standard ΛCDM model.

Acknowledgments

I would like to express my sincere gratitude to Mr. Paul Mitchell for his generous support throughout this project. His guidance in my research, his willingness to answer my many questions, and the time he devoted to helping me work through difficult parts of the process meant a great deal to me. His encouragement and steady support played an important role in the development of this work.

I would also like to thank Mr. Max Henson for his support during the early ideation stage of this project. His willingness to listen carefully to my explanations and engage seriously with my ideas gave me the confidence to continue refining them and to think more critically about their validity.

I am also very grateful to Mr. Dan Miller for taking the time to read my work, for offering honest feedback, and for showing genuine support throughout the process. His kindness, encouragement, and straightforward advice were deeply appreciated and helped me take the work more seriously and continue improving it.

My sincere thanks also go to Dr. Lubomir Bisevac for his professional guidance, for helping me contact other professors, and for sharing thoughtful feedback that helped me reflect more carefully on both the strengths and limitations of this work.

I would also like to express my sincere gratitude to Mrs. Estie Oosthuizen for taking the time to look over my work and for offering such encouraging words. Her support, kindness, and belief in me meant a great deal, and I deeply appreciated her encouragement during this project.

I am also grateful to Kirill Eremenko for taking the time to listen to my thoughts and for offering guidance that helped me think more clearly about the direction of this project. His willingness to engage with my ideas and respond thoughtfully was greatly appreciated, and his support encouraged me to keep developing the work with greater confidence.

I am deeply grateful to Abi Pearson and Leah Jongbloed for their encouragement throughout this journey. Their support meant a great deal during the more difficult stages of the project, and their belief in me helped me continue when the work felt overwhelming.

I would especially like to thank William Morris for his encouragement during some of the most difficult stages of this project. His willingness to listen, offer honest support, and encourage me after setbacks meant a great deal and helped me continue with the work when it became particularly challenging. I remain deeply grateful for his support and for the role he played in helping me persevere.

All feedback, review, guidance, and encouragement acknowledged above were advisory in nature. The final modeling choices, numerical analysis, manuscript revisions, and interpretations presented in this study remained the responsibility of the authors.

Code availability
Code and MATLAB scripts can be accessed at the repository at https://github.com/S0PH1AP/Zero-Sum-Node-Reconfiguration-in-a-Discrete-Spacetime-Substrate

5. References

1. Riess, A. G., Filippenko, A. V., Challis, P., Clocchiatti, A., Diercks, A., Garnavich, P. M., Gilliland, R. L., Hogan, C. J., Jha, S., Kirshner, R. P., Leibundgut, B., Phillips, M. M., Reiss, D., Schmidt, B. P., Schommer, R. A., Smith, R. C., Spyromilio, J., Stubbs, C., Suntzeff, N. B., & Tonry, J. (1998). *Observational evidence from supernovae for an accelerating universe and a cosmological constant*. *The Astronomical Journal, 116*(3), 1009–1038. https://doi.org/10.1086/300499

2. Perlmutter, S., Aldering, G., Goldhaber, G., Knop, R. A., Nugent, P., Castro, P. G., Deustua, S., Fabbro, S., Goobar, A., Groom, D. E., Hook, I. M., Kim, A. G., Kim, M. Y., Lee, J. C., Nunes, N. J., Pain, R., Pennypacker, C. R., Quimby, R., Lidman, C., ... Ellis, R. S. (1999). *Measurements of Ω and Λ from 42 high-redshift supernovae*. *The Astrophysical Journal, 517*(2), 565–586. https://doi.org/10.1086/307221

3. Aghanim, N., Akrami, Y., Ashdown, M., Aumont, J., Baccigalupi, C., Ballardini, M., Banday, A. J., Barreiro, R. B., Bartolo, N., Basak, S., Battye, R., Benabed, K., Bernard, J.-P., Bersanelli, M., Bielewicz, P., Bond, J. R., Borrill, J., Bouchet, F. R., Boulanger, F., & *Planck Collaboration*. (2020). *Planck 2018 results. VI. Cosmological parameters*. *Astronomy & Astrophysics, 641*, A6. https://doi.org/10.1051/0004-6361/201833910

4. Weinberg, D. H., Mortonson, M. J., Eisenstein, D. J., Hirata, C., Riess, A. G., & Rozo, E. (2013). *Observational probes of cosmic acceleration*. *Physics Reports, 530*(2), 87–255. https://doi.org/10.1016/j.physrep.2013.05.001

5. Brout, D., Scolnic, D., Popovic, B., Riess, A. G., Carr, A., Zuntz, J., Kessler, R., Davis, T. M., Hinton, S., Jones, D. O., Rosenthal, K., Peterson, E. R., Murakami, Y., Armstrong, P., Charvu, P., Dwomoh, A., Phillips, M. M., Said, K., Vincenzi, M., … **Pantheon+ Collaboration**. (2022). *The Pantheon+ analysis: Cosmological constraints*. *The Astrophysical Journal, 938*(2), 110. https://doi.org/10.3847/1538-4357/ac8e04

6. Weinberg, S. (1989). *The cosmological constant problem*. *Reviews of Modern Physics, 61*(1), 1–23. https://doi.org/10.1103/RevModPhys.61.1

7. Joyce, A., Jain, B., Khoury, J., & Trodden, M. (2015). *Beyond the cosmological standard model*. *Physics Reports, 568*, 1–98. https://doi.org/10.1016/j.physrep.2014.12.002

8. Bekenstein, J. D. (1973). *Black holes and entropy*. *Physical Review D, 7*(8), 2333–2346. https://doi.org/10.1103/PhysRevD.7.2333

9. Hawking, S. W. (1975). *Particle creation by black holes*. *Communications in Mathematical Physics, 43*(3), 199–220. https://doi.org/10.1007/BF02345020

10. 't Hooft, G. (1993). *Dimensional reduction in quantum gravity*. *arXiv*. https://doi.org/10.48550/arXiv.gr-qc/9310026

11. Susskind, L. (1995). *The world as a hologram*. *Journal of Mathematical Physics, 36*(11), 6377–6396. https://doi.org/10.1063/1.531249

12. Bombelli, L., Lee, J., Meyer, D., & Sorkin, R. D. (1987). *Space-time as a causal set*. *Physical Review Letters, 59*(5), 521–524. https://doi.org/10.1103/PhysRevLett.59.521

13. Yoshiura, S., Takahashi, K., & Takahashi, T. (2020). *Probing small scale primordial power spectrum with 21 cm line global signal*. *Physical Review D, 101*(8), 083520. https://doi.org/10.1103/PhysRevD.101.083520

14. Callen, H. B. (1985). *Thermodynamics and an introduction to thermostatistics* (2nd ed.). Wiley.

15. Pathria, R. K., & Beale, P. D. (2011). *Statistical mechanics* (3rd ed.). Elsevier Academic Press.